Hydrophobic Association of Random Copolymers of Sodium 2-(Acrylamido)-2-methylpropanesulfonate and Dodecyl Methacrylate in Water As Studied by Fluorescence and Dynamic Light Scattering

Tetsuya Noda and Yotaro Morishima*

Department of Macromolecular Science, Graduate School of Science, Osaka University, Toyonaka, Osaka 560-0043, Japan

Received February 16, 1999; Revised Manuscript Received May 16, 1999

ABSTRACT: The association behavior of random copolymers of sodium 2-(acrylamido)-2-methylpropanesulfonate (AMPS) and dodecyl methacrylate (DMA) with its content (f_{DMA}) varying from 1 to 15 mol % was investigated by fluorescence and quasielastic light scattering (QELS) techniques in 0.1 M NaCl aqueous solutions. The association behavior of the copolymers was found to depend strongly on f_{DMA}. When $f_{DMA} < 3$ mol %, some polymer chains exist as unimers with a hydrodynamic radius (R_h) of about 5 nm while some polymers form multipolymer aggregates with $R_h \approx 100$ nm, arising from "hydrophobic cross-linking" by the interpolymer association of dodecyl groups. When f_{DMA} is increased to 9 mol %, interpolymer hydrophobe associations lead to the formation of a multipolymer micelle with $R_h \approx 10-13$ nm. The aggregation number (N_{agg}) of dodecyl groups in a micelle core was estimated to be about 195. When f_{DMA} is further increased to 15 mol %, R_h for the multipolymer micelle markedly increases to 70−180 nm, the size increasing with increasing polymer concentration, whereas N_{agg} remains constant at about 158 independent of the polymer concentration. On the basis of the results from the fluorescence and QELS measurements, a unicore micelle model was proposed for the copolymer with $f_{DMA} = 9$ mol %, and a bridged micelle model was proposed for the copolymer with $f_{DMA} = 15$ mol %.

Introduction

The association behavior of hydrophobically modified water-soluble polymers in aqueous solution has been a target of extensive studies over the past decades in part because of its relevance to biological phenomena and in part because of its importance in practical applications.[1−11] The association of polymer-bound hydrophobes may occur either between different polymer chains or within a single polymer chain or both at a time. Interpolymer hydrophobe association may lead to gelation or phase separation (i.e., precipitation), whereas intrapolymer association may lead to the formation of single-molecular micelles (unimer micelles).

The hydrophilic−hydrophobic balance of polymer molecules is a primarily important factor to determine the association behavior of amphiphilic polymers. In the case of hydrophobically modified polyelectrolytes, the balance of the numbers of hydrophobes and charge in a polymer chain is particularly important for hydrophobe associations because hydrophobic interactions would compete with electrostatic repulsions. Experimental results reported so far indicate that the type of hydrophobes, their content in a polymer, the sequence distribution of electrolyte and hydrophobic monomer units in a polymer chain, and the type of spacer bonding between hydrophobes and the polymer chain are some of the structural parameters that determine whether intra- or interpolymer hydrophobic association occurs preferentially.[12−21]

The association behavior is a strong function of the content of hydrophobes in a polymer. The maximum amount of hydrophobes that can be incorporated into a polymer chain, while keeping the polymer soluble in water, strongly depends also on the structural parameters just described. For instance, random copolymers

Chart 1. Chemical Structure of Copolymers Studied

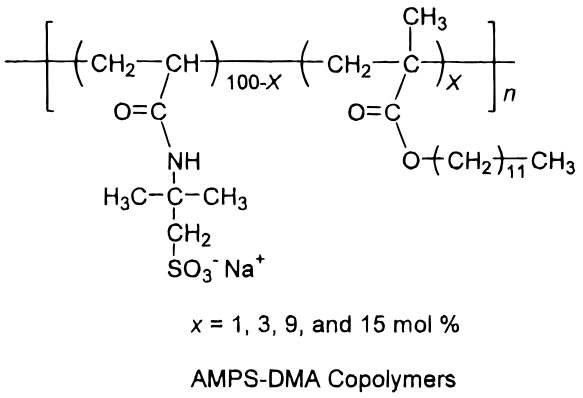

x = 1, 3, 9, and 15 mol %

AMPS-DMA Copolymers

of sodium 2-(acrylamido)-2-methylpropanesulfonate (AMPS) and *N*-dodecyl-, *N*-cyclododecyl-, or *N*-adamantylmethacrylamide are soluble in water up to about 60 mol % of the hydrophobic methacrylamide content.[20,22−29] In contrast, we found, in the present study, that random copolymers of AMPS and dodecyl methacrylate (DMA) (Chart 1) were soluble in water only when the content of the DMA unit in the copolymer (f_{DMA}) was as low as 15 mol %. Thus, there is a great difference in the solubility in water between the AMPS copolymers possessing amide- and ester-linked hydrophobes.

There is a general tendency that interpolymer association is favorable in concentrated solutions whereas intrapolymer association is favorable in dilute solutions. The AMPS copolymers with the hydrophobic methacrylamides form unimer micelles in aqueous solutions even at very high polymer concentrations, arising from predominant intrapolymer association of pendant hydrophobes independent of the polymer concentration.[24−29] In contrast, random copolymers of AMPS and a choles-

10.1021/ma990202j CCC: $18.00 © 1999 American Chemical Society
Published on Web 06/24/1999

terol-bearing methacrylate, cholesteryl 6-methacryloyloxyhexanoate, in aqueous solution showed a strong tendency for interpolymer association,[21] and an intermolecularly bridged "flowerlike" micelle has been proposed on the basis of the model proposed by Halperin[30] and Semenov et al.[31] These contrasting behavior of the two AMPS copolymers is a clear indication of the large effect of structural variations in the side chains of hydrophobic monomer units on the association behavior of AMPS copolymers.

These results of our earlier studies motivated us to investigate the association behavior of random copolymers of AMPS and DMA, an ester-linked hydrophobic monomer, as a function of f_{DMA} over a wide range of the polymer concentration in aqueous solution with the aim of further clarifying the effect of spacer bonding on the hydrophobe association. Various fluorescence probe techniques, using pyrene, and quasielastic light scattering (QELS) techniques were employed to monitor hydrophobe associations. On the basis of experimental results, we proposed a conceptual model for the hydrophobe associations of AMPS−DMA copolymers with varying f_{DMA}.

Experimental Section

Materials. Dodecyl methacrylate (DMA), purchased from Aldrich Chemical Co., was distilled under reduced pressure. 2-(Acrylamido)-2-methylpropanesulfonic acid (AMPS), purchased from Wako Pure Chemical Co., was used without further purification. 2,2′-Azobis(isobutyronitrile) (AIBN) was recrystallized from ethanol. Pyrene was recrystallized twice from ethanol. Water was purified with a Millipore Milli-Q system. Other reagents were used as received.

Polymers. The copolymers of AMPS and DMA were prepared by free radical copolymerization in the presence of AIBN in *N*,*N*-dimethylformamide (DMF). A representative procedure for the copolymerization is as follows: A known amount of AMPS was neutralized by equinormal Na_2CO_3 in DMF, and predetermined amounts of DMA and AIBN were added to this solution. The mixture was placed in a glass ampule and outgassed on a high-vacuum line by six freeze−pump−thaw cycles, and the ampule was vacuum-sealed. Polymerization was carried out at 60 °C for 21 h. The polymerization mixture was poured into a large excess of diethyl ether to precipitate the resulting polymer. The polymer was purified by reprecipitation from methanol into a large excess of diethyl ether three times and then dissolved in pure water. The aqueous solution was dialyzed against pure water for a week, and the polymer was recovered by a freeze-drying technique. The composition of the copolymer was determined by ^{1}H NMR spectroscopy.

Measurements. a. NMR. ^{1}H NMR spectra were measured with a JEOL GSX-400 NMR spectrometer using D_2O as a solvent at 65 °C. Chemical shifts were determined by using TMS as an internal standard.

b. Gel Permeation Chromatography (GPC). Measurements were performed at 60 °C with a JASCO GPC-900 instrument equipped with an Asahipak GF-7M HQ column (Shodex) in combination with JASCO UV-975 and RI-930 detectors. A 0.2 M phosphate buffer solution containing 50% (v/v) acetonitrile (HPLC grade purchased from Wako Pure Chemicals) was used as an eluent. Molecular weights of polymers were calibrated by standard sodium poly(styrenesulfonate) (Polyscience Inc.) and standard pullulan (Shodex standard P-82) samples. For all the measurements, the elution rates were fixed to 1.0 mL/min.

c. Absorption Spectra. Absorption spectra were recorded on a JASCO V-550 spectrophotometer using a 1.0 cm path length quartz cell. Pyrene concentrations in polymer aqueous solutions were estimated by absorbances at 334 nm using $\epsilon_{334} = 54\,000\ M^{-1}\ cm^{-1}$ in water.[32]

d. Fluorescence. *(1) Steady-State Fluorescence Measurements.* Steady-state fluorescence spectra were recorded on a Hitachi F-4500 fluorescence spectrophotometer. Emission spectra of pyrene were measured with excitation at 338 nm at room temperature. Excitation spectra were monitored at 372 nm. The slit widths for both the excitation and emission side were kept at 2.5 nm during measurement. Sample solutions were prepared by dissolving a known amount of polymer in a pyrene-saturated water, and the solutions were allowed to stand for 1 day for equilibration. Pyrene-saturated water was prepared as reported previously.[21]

For the determination of the critical micelle concentration (cmc) of the polymers, excitation spectra of pyrene were measured at varying concentrations of the polymers, as reported by Wilhelm et al.[33]

(2) Time-Resolved Fluorescence Measurements. Fluorescence decay data were collected on a HORIBA NAES 550 system equipped with a flash lamp filled with hydrogen. Sample solutions containing pyrene probes were excited at 338 nm, and pyrene fluorescence was monitored around 400 nm with a band-pass filter (Toshiba KL-40) and a cutoff filter (Toshiba L-38) placed between the sample and detector. Sample solutions were prepared as described above and purged with Ar for about 30 min prior to measurement. Measurements were performed with a pyrene concentration of 4×10^{-7} M. No excimer formation was confirmed at this pyrene concentration by steady-state fluorescence measurements in the absence and presence of the polymers. The observed decay is a convolution of the sample decay function and the instrumental response function. Fluorescence decay data were fitted to a single- or double-exponential function. For criteria for the goodness of the fit, χ^2 and the weighted residuals were used.

Aggregation numbers (N_{agg}) of polymer-bound hydrophobes were determined using pyrene probes. Pyrene molecules were solubilized in the polymer micelle at high concentrations such that excimer was formed in the micelle. Sample solutions were prepared by pouring a small amount of a concentrated pyrene solution in acetone into aqueous solutions of the polymer. All sample solutions were filtered with a 0.2 μm membrane filter prior to measurement. The determination of N_{agg} is based on the Infelta−Tachiya equation for quenching in monodisperse micelles.[34,35] In the present study, the quenching of pyrene monomer fluorescence, arising from excimer formation, was used to determine N_{agg}. Fluorescence decay data were fitted to the following equation:

$$\ln[I(t)/I(0)] = A_3[\exp(-A_4 t) - 1] - A_2 t \qquad (1)$$

where $I(t)$ and $I(0)$ are the fluorescence intensities at time t and 0 following excitation, respectively. Parameters A_2, A_3, and A_4 are determined from the best fit. In the case where the distributions of fluorescence probe molecules over the micelles are frozen on the time scale of the fluorescence lifetime, these three parameters are expressed as

$$A_2 = k_0, \quad A_3 = [Q]_m/[M], \quad A_4 = k_Q \qquad (2)$$

where k_0 (i.e., τ_0^{-1}) is the fluorescence decay rate constant for pyrene inside the micelle without excimer formation, $[Q]_m$ is the molar concentrations of quencher inside micelles, and [M] is the molar concentration of micelles. k_Q is the pseudo-first-order rate constant for quenching of the excited probe. Because the quenching of pyrene monomer fluorescence is due to the excimer formation of pyrene, $[Q]_m$ corresponds to the concentration of pyrene.[36,37] N_{agg} is calculated from A_3 and

$$N_{agg} = [\text{hydrophobe}]/[M] \qquad (3)$$

where [hydrophobe] is the molar concentration of polymer hydrophobes which can be calculated from the polymer concentration and the content of the hydrophobe in the polymer as

$$[\text{hydrophobe}] = [\text{polymer}]\ (g/L) \times \{\text{content of hydrophobe}\}\ (mol/g) \qquad (4)$$

e. Quasielastic Light Scattering (QELS). QELS data were obtained at 25 ± 0.1 °C with an Otsuka Electronics Photal DLS-700 light scattering spectrometer equipped with an Ar laser (60 mW at 488 nm) and a ALV-5000, multi-τ digital time correlator. All sample solutions of polymer in water were filtered with a 0.2 μm membrane filter prior to measurement. The observed intensity autocorrelation function, $g^{(2)}(t)$, was related to the normalized auto correlation function, $g^{(1)}(t)$, by the Siegert relation

$$g^{(2)}(t) = B[1 + \beta\,|g^{(1)}(t)|^2] \tag{5}$$

where β is a constant parameter for the optical system and B is a baseline term. To obtain the relaxation time distribution, $\tau A(\tau)$, the inverse Laplace transform (ILT) analysis for the intensity autocorrelation function was performed by conforming the REPES algorithm,[38] as follows:

$$g^{(1)}(t) = \tau A(\tau)\exp(-t/\tau)\,\mathrm{d}\ln\tau \tag{6}$$

The relaxation time distributions are given as a $\tau A(\tau)$ versus log τ profile with an equal area.

Diffusion coefficients, D, are calculated from the ILT moments as $D = (\Gamma/q^2)_{q\to 0}$, where q is the magnitude of scattering vector expressed as $q = (4\pi n/\lambda)\sin(\theta/2)$ where n is the index of refraction of the solution. The hydrodynamic radius, R_h, is given by the Einstein−Stokes equation:

$$R_h = k_B T/6\pi\eta D \tag{7}$$

where k_B is the Boltzmann constant, T is the absolute temperature, and η is the solvent viscosity. The details of QELS instrumentation and theory are described in the literature.[39]

f. Transmission Electron Micrograph (TEM). Electron micrographs were taken with a JEOL JEM-1200 EX-II transmission electron microscope at 60 kV. An aqueous polymer solution (polymer concentration was about 0.01 wt %) was applied to a 400 mesh nickel grid covered with a poly(vinyl formal) film followed by air-drying. The cast film was stained by applying a drop of a 2.0 wt % aqueous solution of uranyl acetate. The specimen thus prepared was observed at a direct magnification of (2.5−10) × 10^4.

Results and Discussion

Characterization of Copolymers. Figure 1 shows ^{1}H NMR spectra for the AMPS−DMA copolymers prepared with varying mole ratios of AMPS and DMA in the monomer feed. All the NMR spectra were measured with a polymer concentration of 10 g/L in D_2O at 65 °C. On the basis of the ratios of the area intensities of the resonance peaks around 1.0 and 3.5 ppm due to the methyl protons in the dodecyl group in DMA and methylene protons in AMPS, respectively, the contents of DMA, f_{DMA}, in the four copolymers were estimated to be about 1, 3, 9, and 15 mol %. AMPS−DMA copolymers of higher f_{DMA} were also synthesized, but the copolymers with f_{DMA} > 15 mol % were found to be insoluble in water and therefore were not used for further studies.

The molecular weights of the copolymers with f_{DMA} ≤ 15 mol % were estimated by GPC calibrated with standard pullulan and sodium poly(styrenesulfonate) samples in a 0.2 M phosphate buffer solution containing 50% (v/v) acetonitrile (Table 1). In this water/acetonitrile (1/1, v/v) mixed solvent, hydrophobic interactions are virtually absent.[21] These four copolymers have similar number- and weight-average molecular weights on the order of 10^4 and similar molecular weight distributions (M_w/M_n). We attempted to determine M_w by static light scattering (SLS) in 0.1 M NaCl aqueous solutions but failed to calculate M_w because Zimm plots were considerably curved, suggesting the presence of interpolymer associations in aqueous solutions. On the basis of the DMA content and the molecular weight, the number of DMA units per polymer can be roughly calculated to be about 2, 6, 18, and 35 for the copolymers with f_{DMA} = 1, 3, 9, and 15 mol %, respectively.

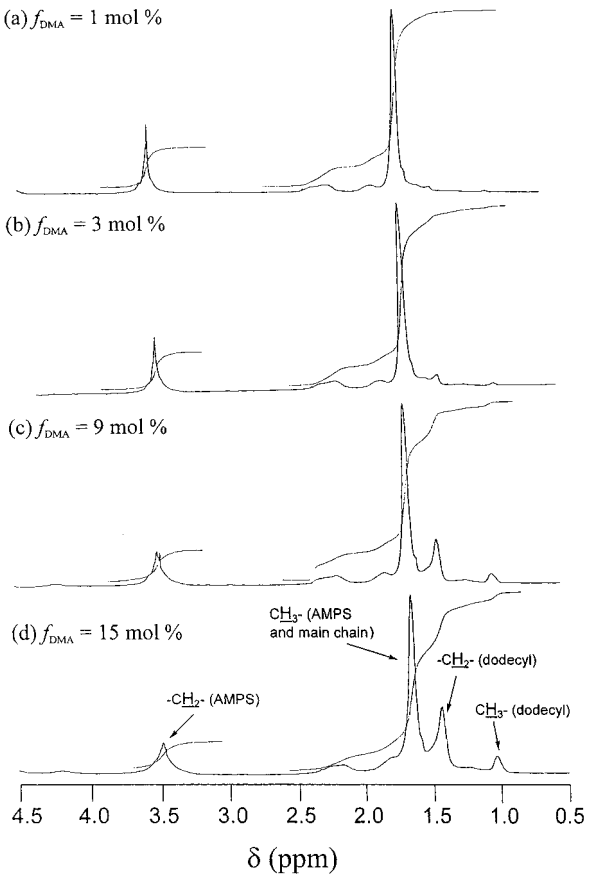

Figure 1. The 400 MHz ^{1}H NMR spectra for the copolymers in D_2O at 65 °C.

Table 1. Characteristics of the Copolymers

f_{DMA}[a] (mol %)	M_w[b] (10^4)	M_w/M_n[b]	no. of dodecyl group per polymer chain	cmc[c] (g/L)	K_v[d]
1	5.4	2.5	2	9.0	2.3×10^3
3	4.6	3.1	6	1.9	2.4×10^3
9	4.2	2.5	18	0.04	2.8×10^4
15	5.0	2.9	35	0.01	8.1×10^4

[a] Mole percent content of DMA in the copolymer determined by ^{1}H NMR. [b] Determined by GPC using a 0.2 M phosphate buffer solution containing 50% (v/v) acetonitrile. [c] Determined from steady-state fluorescence excitation spectra of pyrene probes (see text). [d] Partition coefficient for pyrene (see text).

Hydrophobic Microdomains Formed by Dodecyl Groups. Molecular pyrene is a useful fluorescence probe for characterization of molecular assemblies of numerous surfactants and associating polymers.[33,40−43] It is well-established that the steady-state fluorescence intensity and fluorescence lifetime for pyrene reflect the polarity of media where the pyrene probe exists, the intensity and the lifetime increasing with decreasing the environmental polarity.[40] Furthermore, the relative intensity of the third to first vibrational peaks, I_3/I_1, in pyrene fluorescence spectra is known to be sensitive to the micropolarity of the local environment, the ratio increasing with decreasing environmental polarity.[40]

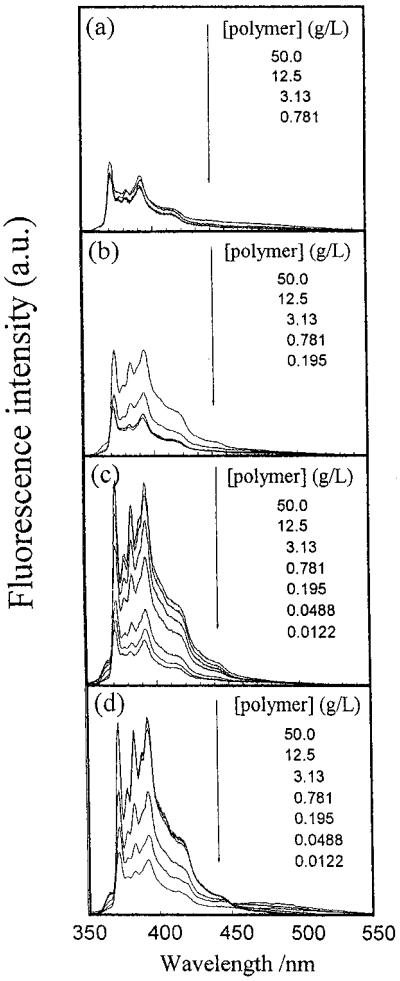

Figure 2. Steady-state fluorescence emission spectra for pyrene in 0.1 M NaCl aqueous solution in the presence of varying concentrations of the copolymers with $f_{DMA} = 1$ (a), 3 (b), 9 (c), and 15 mol % (d). Excitation wavelength: 338 nm.

Figure 2 shows steady-state fluorescence spectra of pyrene probes dissolved in 0.1 M NaCl aqueous solutions in the presence of the copolymers of different f_{DMA} at varying concentrations. In all measurements, the concentration of pyrene was adjusted to 4×10^{-7} M. The fluorescence intensity depends strongly on the polymer concentration and also on f_{DMA}, indicating that pyrene probes are solubilized in polymer phases. The fluorescence spectra reflect the partition of pyrene molecules between the aqueous bulk and polymer phases as well as the micropolarity of the polymer phase. In the case of the copolymer with $f_{DMA} = 1$ mol %, the fluorescence intensities are practically the same in the whole range of the copolymer concentrations studied. For the copolymers of $f_{DMA} > 3$ mol %, however, the fluorescence intensity increases with an increase in the polymer concentration. This tendency is more significant for the copolymers with higher f_{DMA}. These results indicate that dodecyl groups in the copolymers associate and form hydrophobic microdomains in which pyrene molecules are solubilized.

In Figure 3, the I_3/I_1 ratios for all the copolymers are plotted against the polymer concentration. At the lowest polymer concentration (10^{-3} g/L), the I_3/I_1 ratios for all the copolymers are in the neighborhood of 0.6, which is practically the same as that for pyrene in water.[40] As the polymer concentration is increased, the I_3/I_1 ratio begins to increase significantly at a certain polymer

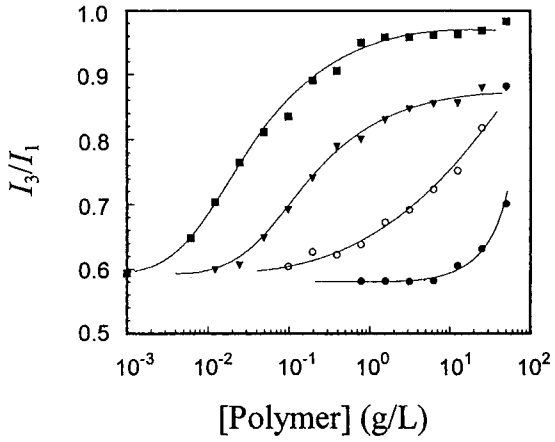

Figure 3. Plots of the I_3/I_1 ratio as a function of the polymer concentration for the copolymers with varying f_{DMA}. $f_{DMA} = 1$ (●), 3 (○), 9 (▼), and 15 mol % (■).

concentration. The polymer concentration for the onset of the increase in the I_3/I_1 ratio upon an increase in the polymer concentration depends strongly on f_{DMA}, and this onset polymer concentration is much lower for higher f_{DMA}. In the case of $f_{DMA} = 15$ mol %, the I_3/I_1 ratio begins to increase at a polymer concentration of $\sim 10^{-2}$ g/L, reaching a constant value of $I_3/I_1 \approx 0.95$ near 1 g/L polymer. The onset polymer concentration for $f_{DMA} = 9$ mol % is nearly 1 order of magnitude higher than that for $f_{DMA} = 15$ mol %. For the copolymers with $f_{DMA} = 3$ and 1 mol %, the onset polymer concentrations are more than 1 and 2 orders of magnitude higher than that for the copolymer with $f_{DMA} = 9$ mol %, respectively.

Critical Micelle Concentration (cmc). The aggregates of the polymers, consisting of hydrophobic microdomains surrounded by charged segments, may be viewed as a polymer micelle. As in the case of small molecular weight surfactant micelles, the formation of the polymer micelle may occur at a certain critical polymer concentration. If that is the case, we may define such a critical polymer concentration as a cmc for micelle-forming polymers.

We attempted to estimate an apparent cmc for the present copolymers by a fluorescence method reported by Wilheim et al.[33] This method is based on the fact that the pyrene 0−0 absorption band shifts toward longer wavelengths when pyrene is solubilized in a hydrophobic phase in a micelle. For example, the 0−0 absorption maximum of pyrene in water is at 334 nm whereas it shifts to 338 nm when pyrene is solubilized in micelles of polystyrene-*b*-poly(ethylene oxide)[33] or polystyrene-*b*-poly(sodium acrylate).[44]

Figure 4 shows excitation spectra for pyrene probes dissolved in 0.1 M NaCl aqueous solutions in the presence of the AMPS−DMA copolymers of varying f_{DMA} at varying polymer concentrations, measured at a constant pyrene concentration of 4×10^{-7} M. The 0−0 absorption band for pyrene solubilized in hydrophobic microdomains formed by the copolymers was observed at 337 nm. The ratio of the intensity at 337 nm relative to that at 334 nm (I_{337}/I_{334}) is plotted against the polymer concentration in Figure 5. Upon an increase in the polymer concentration, the I_{337}/I_{334} ratio for each copolymer exhibits a significant increase at a certain polymer concentration. Pyrene probes can exist either in the polymer micellar phase or in the bulk aqueous phase. The ratio of the pyrene concentrations in the micellar phase and in the aqueous phase, $[Py]_m/[Py]_w$,

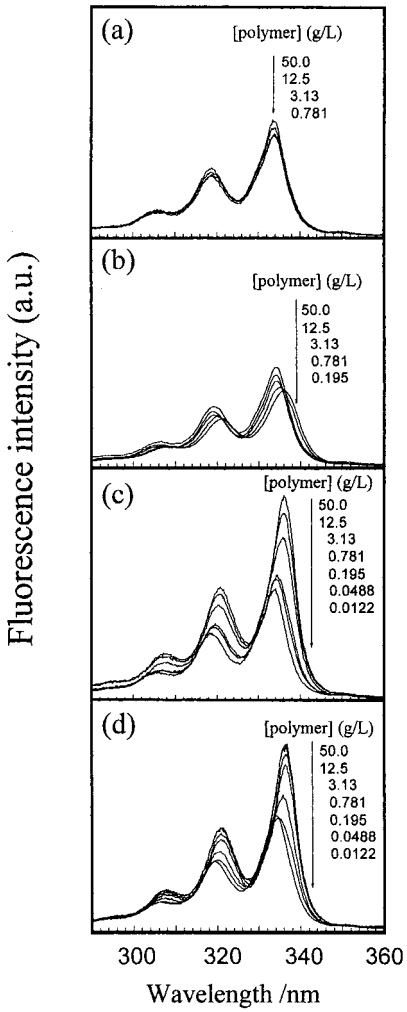

Figure 4. Steady-state fluorescence excitation spectra for pyrene at varying polymer concentrations in 0.1 M NaCl aqueous solutions monitored at 372 nm.

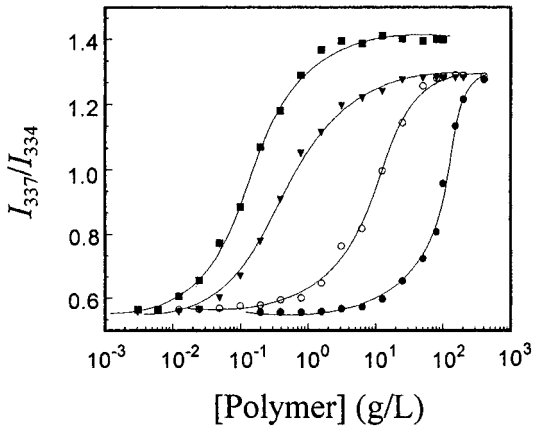

Figure 5. Relationship between the I_{337}/I_{334} ratio and the polymer concentration. f_{DMA} = 1 (●), 3 (○), 9 (▼), and 15 mol % (■).

can be calculated by

$$[Py]_m/[Py]_w = \{(I_{337}/I_{334}) - (I_{337}/I_{334})_{min}\}/\{(I_{337}/I_{334})_{max} - (I_{337}/I_{334})\} \quad (8)$$

where $(I_{337}/I_{334})_{min}$ and $(I_{337}/I_{334})_{max}$ are the minimum and maximum values for the I_{337}/I_{334} ratio that can be estimated from Figure 5. On the other hand, the $[Py]_m/[Py]_w$ ratio can be expressed as

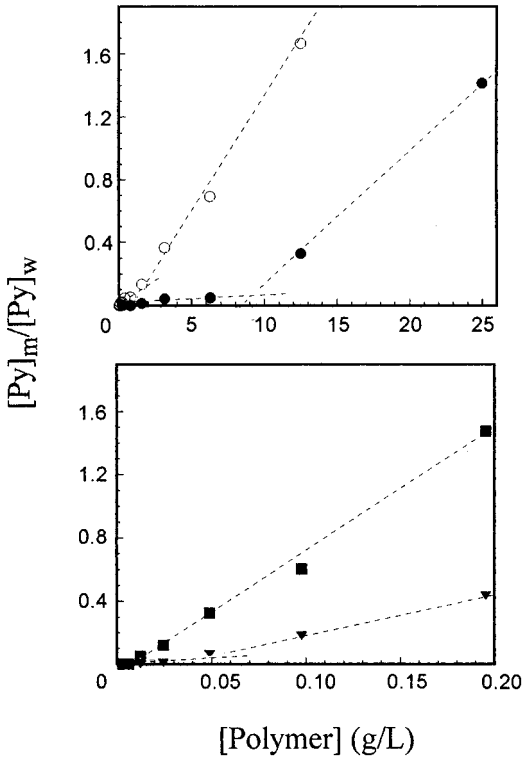

Figure 6. Plots of $[Py]_m/[Py]_w$ estimated from the I_{337}/I_{334} ratio against the polymer concentration with varying f_{DMA}. f_{DMA} = 1 (●), 3 (○), 9 (▼), and 15 mol % (■).

$$[Py]_m/[Py]_w = K_v\chi_{Dod}(c - cmc)/1000\rho_{Dod} \quad (9)$$

where K_v is the partition coefficient, χ_{Dod} is the weight fraction of the dodecyl unit in the copolymer that can be calculated from f_{DMA}, and ρ_{Dod} is the density of the dodecyl domain in the micelle. We assume that ρ_{Dod} is the same as that of dodecane (0.751 g/mL at 20 °C).

Figure 6 shows plots of $[Py]_m/[Py]_w$ against the polymer concentration. For these plots we used $(I_{337}/I_{334})_{min}$ = 0.558 for all the copolymers and $(I_{337}/I_{334})_{max}$ = 1.28 and 1.40 for f_{DMA} = 1−9 and 15 mol %, respectively. From the intercept of the sloping lines on the abscissa, cmc values are estimated as listed in Table 1. The value of cmc depends strongly on f_{DMA}; for f_{DMA} = 1 mol %, an apparent cmc is 9.0 g/L, whereas for f_{DMA} = 15 mol %, it decreases down to the order of 10^{-2} g/L. The partition coefficients for the copolymers were estimated from the slope of the straight line above cmc in Figure 6 as listed in Table 1. The large K_v values on the order of 10^4 suggest that the onset of the increase in the I_{337}/I_{334} ratio in Figure 5 corresponds to the onset of the hydrophobic microdomain formation and does not reflect an increment of the number of the hydrophobic microdomains with an increase in the polymer concentration. The cmc values thus estimated are close to the polymer concentrations for the onset of the increases in the I_3/I_1 ratio (Figure 3).

Aggregation Number (N_{agg}) of Dodecyl Groups. The aggregation number N_{agg} of polymer-bound hydrophobes is an important parameter to characterize polymer micelles. Various experimental methods for the determination of N_{agg} have been reported,[42] which include ultrasonic relaxation,[45] light scattering,[46] small-angle neutron scattering,[47] and fluorescence[48] techniques. In the present study, we attempted to determine

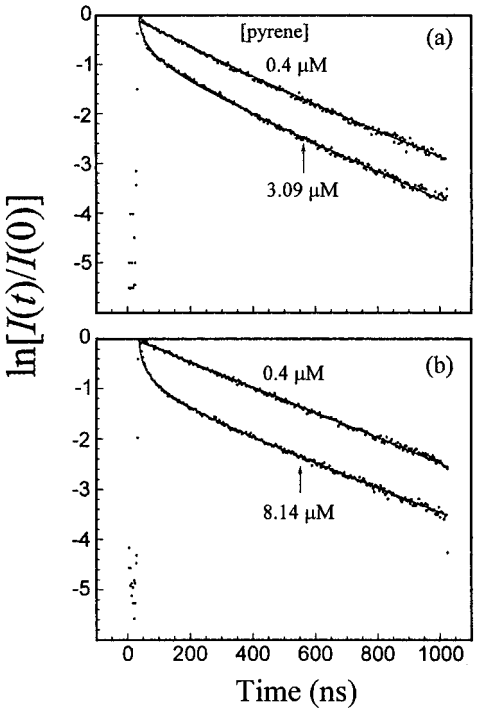

Figure 7. Comparison of fluorescence decays at different concentrations of pyrene in the presence of the copolymers (1.56 g/L) with $f_{DMA} = 9$ (a) and 15 mol % (b) in 0.1 M NaCl aqueous solution.

N_{agg} of dodecyl groups in the copolymers employing a fluorescence technique based on the excimer formation of pyrene molecules solubilized in the hydrophobic microdomains of the polymers, as described in detail in the Experimental Section.[34,35,47,48] For the calculation of N_{agg}, we assumed that all pyrene molecules were randomly distributed over the hydrophobic microdomains according to a Poisson distribution.

Figure 7 shows examples of fluorescence decay data for the copolymers with $f_{DMA} = 9$ and 15 mol % at a polymer concentration of 1.56 g/L in 0.1 M NaCl aqueous solutions. In the absence of the copolymer, a 0.4 μM pyrene solution in 0.1 M NaCl shows a single-exponential fluorescence decay with a lifetime of 191 ns ($\chi^2 = 1.07$). In the presence of the copolymer of $f_{DMA} = 15$ mol % (1.56 g/L), the decay is single-exponential with a fluorescence lifetime of 404 ns ($\chi^2 = 1.21$). In the case of the copolymer of $f_{DMA} = 9$ mol % (1.56 g/L), however, the fluorescence decay is nearly single-exponential but better fitted to a double-exponential function with a major decay component for a lifetime of 395 ns and a very minor component for 191 ns, suggesting that a small fraction of pyrene molecules exists in the bulk aqueous phase and contributes to the fluorescence decay observed.

When the concentration of solubilized pyrene is very low such that each hydrophobic microdomain contains less than one pyrene molecule on average, no excimer is formed. However, when the average number of pyrene molecules solubilized in a hydrophobic microdomain is two or more, excimer would be formed within the hydrophobic microdomain, leading to a fast decay component in the decay of monomeric pyrene fluorescence. In Figure 7, fluorescence decays observed at higher concentrations of pyrene are also presented, i.e., 3.09 and 8.14 μM pyrene for the copolymers with $f_{DMA} = 9$ and 15 mol %, respectively. These decay data are best-fitted to eq 1 with $\chi^2 = 1.25$ and 1.10 for the copolymers with $f_{DMA} = 9$ and 15 mol %, respectively. From the best fit, parameters A_2, A_3, and A_4 in eq 1 can be determined, thus allowing us to calculate N_{agg} of dodecyl groups using eqs 3 and 4. These results are listed in Table 2 together with the results obtained at several different concentrations of the polymer and pyrene. Within the concentration ranges of the polymer and pyrene studied, all the fitting parameters including k_Q are practically independent of the concentrations of the polymer and pyrene. Namely, there is no particular dependence of N_{agg} on the concentrations of the polymer and the probe. Therefore, we averaged N_{agg} values obtained (Table 2). For the copolymer with $f_{DMA} = 9$ mol %, the average N_{agg} value is 195, observed values ranging from 169 to 211. For the copolymer with $f_{DMA} = 15$ mol %, the average N_{agg} value is 158, a little smaller than that for $f_{DMA} = 9$ mol %, observed values ranging from 151 to 163. From the molecular weight and f_{DMA}, the number of dodecyl groups per polymer chain can be calculated to be 18 and 35 for the copolymers of $f_{DMA} = 9$ and 15 mol %, respectively (Table 1). If we assume that one polymer micelle has one hydrophobic domain (i.e., a unicore micelle), the polymer aggregation number can be estimated to be about 11 and 4−5 for the copolymers of $f_{DMA} = 9$ and 15 mol %. We will discuss this point in more detail in the following subsection.

Table 2. Fitting Parameters for Eq 1 and Aggregation Numbers of Dodecyl Groups in the Hydrophobic Microdomain

f_{DMA} (mol %)	[polymer] (g/L)	[pyrene][a] (μM)	A_3	$10^{-6}k_Q$ (s^{-1})	A_2^{-1} (ns)	χ^2	N_{agg}
9	1.56	3.09	0.786	19.8	337	1.25	169
	0.781	1.75	1.11	23.8	334	1.26	211
	0.391	0.889	1.12	21.0	314	1.19	210
	0.195	0.555	1.26	19.2	301	1.20	188
						av	195
15	1.56	8.14	1.19	20.1	340	1.10	160
	0.781	3.58	0.990	25.4	349	1.21	151
	0.391	1.82	1.09	24.3	302	1.02	163
						av	158

[a] Concentrations were calculated from the absorbance at 334 nm using $\epsilon_{334} = 54\,000$ M^{-1} cm^{-1}.[32]

Hydrodynamic Size of the Polymer Aggregates. Figure 8 compares relaxation time distributions in QELS for the copolymers with varying f_{DMA} at three polymer concentrations in 0.1 M NaCl. In the case of $f_{DMA} = 1$ mol %, the relaxation time distributions were found to be bimodal with a fast and slow mode relaxation peaks. With an increase in the polymer concentration, the height of the slow mode peak relative to that of the fast mode peak increases. The copolymer with $f_{DMA} = 3$ mol % also exhibits a bimodal distribution although the slow mode distribution appears as a shoulder at the lowest polymer concentration (0.781 g/L). The relaxation time distribution for this polymer is similarly dependent on the polymer concentration as in the case of $f_{DMA} = 1$ mol %. These observations are a manifestation of interpolymer hydrophobe associations, leading to the formation of multipolymer aggregates.

We measured the relaxation time distributions at varying scattering angles, and the relaxation rate (Γ) (i.e., the reciprocal of the relaxation time) at each peak top was plotted against q^2, the plot giving a straight line passing through the origin (data not shown). From the diffusion coefficient (D) estimated from the slope of the plot, apparent hydrodynamic radii (R_h) for the fast

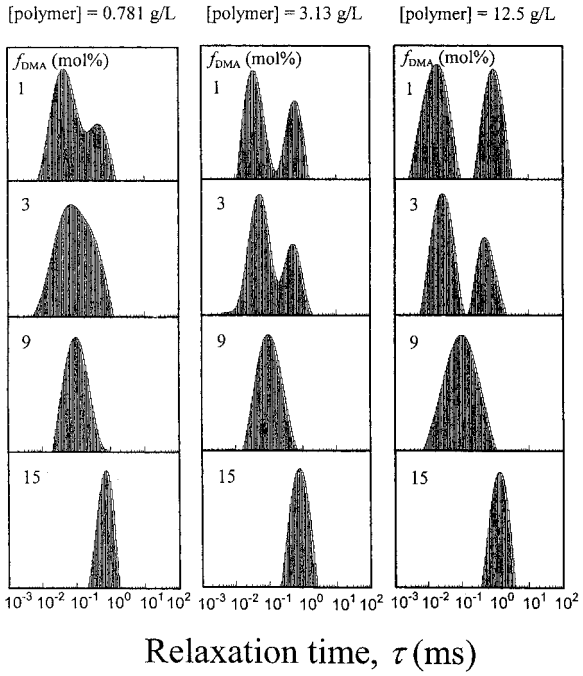

Figure 8. Relaxation time distributions for the copolymers with varying f_{DMA} at varying polymer concentrations.

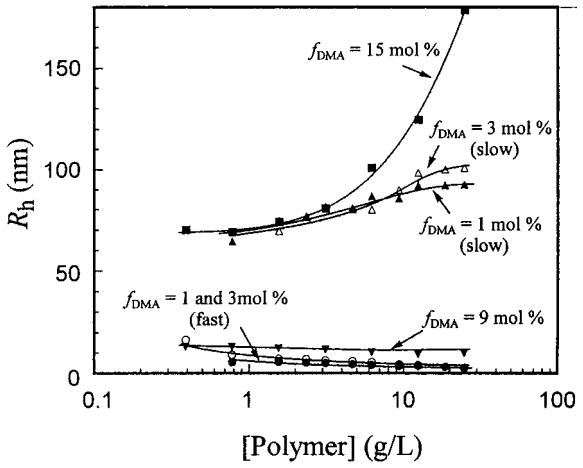

Figure 9. Relationship between R_h and the polymer concentration.

and slow relaxation modes were calculated from eq 7 (see Experimental Section). Values of R_h thus estimated for the copolymers of f_{DMA} = 1 and 3 mol % are plotted against the polymer concentration in Figure 9. The R_h values for the fast mode component are within a range of 4−6 nm regardless of the polymer concentration. On the other hand, the R_h values for the slow mode component are about 70 nm at a polymer concentration of 0.5 g/L and increase to 90−100 nm as the polymer concentration is increased to 25 g/L. In addition, as can be seen from Figure 8, the component of the slow mode relative to that of the fast mode increases with increasing polymer concentration. This ratio for f_{DMA} = 1 mol % is larger than that for f_{DMA} = 3 mol % at any polymer concentrations. As f_{DMA} is increased to 9 mol %, the relaxation time distributions become apparently unimodal (Figure 8). The diffusion coefficients were estimated from the slope of $\Gamma - q^2$ plots as described above, from which R_h values were calculated using eq 7. The R_h values thus calculated for the copolymer with f_{DMA} = 9 mol % are in a range of 10−13 nm within the range

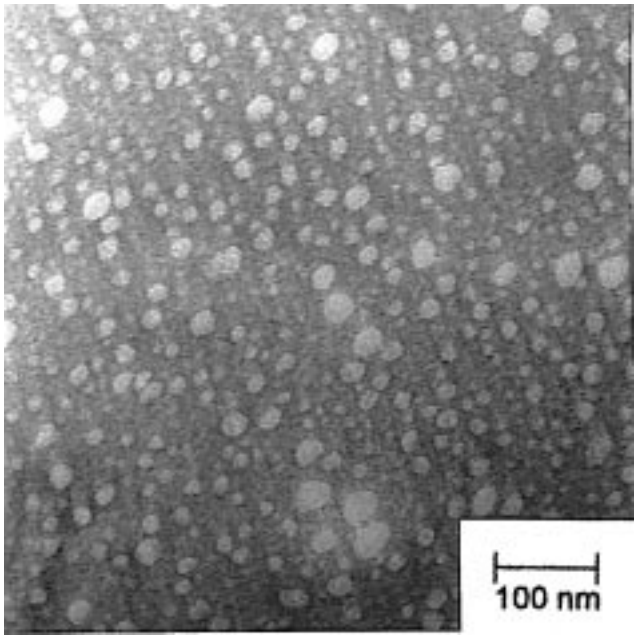

Figure 10. TEM image of the copolymer with f_{DMA} = 9 mol %.

of the polymer concentration from 0.313 to 25.0 g/L (Figure 9). As f_{DMA} is increased to 15 mol %, the fast mode component disappears completely, and the distribution becomes very narrow (Figure 8). The R_h values estimated for the copolymer with f_{DMA} = 15 mol % are in a range of 70−180 nm in the same range of the polymer concentrations, R_h increasing with an increase in the polymer concentration as can be seen in Figure 9.

These results indicate that the AMPS−DMA copolymers have a strong tendency for interpolymer hydrophobe associations and that the association behavior is very much different for different DMA contents in the copolymer. The slow mode observed for the copolymers with f_{DMA} = 1 and 3 mol % is obviously due to interpolymer aggregates, and the fast mode is likely to be due to single polymers (i.e., unimers). It is a surprising observation that the copolymer exhibits a tendency for interpolymer association even at f_{DMA} as low as 1 mol %. When f_{DMA} is increased to 9 mol %, all polymer chains exist as interpolymer aggregates, but their sizes are much smaller than those observed for f_{DMA} = 1 and 3 mol % and do not increase when the polymer concentration is increased. When f_{DMA} is further increased to 15 mol %, however, the association behavior is completely different from that of the copolymer with f_{DMA} = 9 mol %; i.e., all polymer chains form much larger aggregates, and the sizes of the aggregates increase with the polymer concentration.

The results described above suggest that the interpolymer aggregates formed by the copolymer of f_{DMA} = 9 mol % may be multipolymer micelles with well-defined shape and size independent of the polymer concentration. As can be seen from a TEM image presented in Figure 10, spherical objects whose apparent radii ranging from 5 to 15 nm are clearly observed. On the basis of the size and shape of these objects, we conclude that they are multipolymer micelles formed by the copolymer of f_{DMA} = 9 mol %.

It is important to point out here that the association behavior of the AMPS−DMA copolymers is dramatically different from that of the random copolymers of AMPS

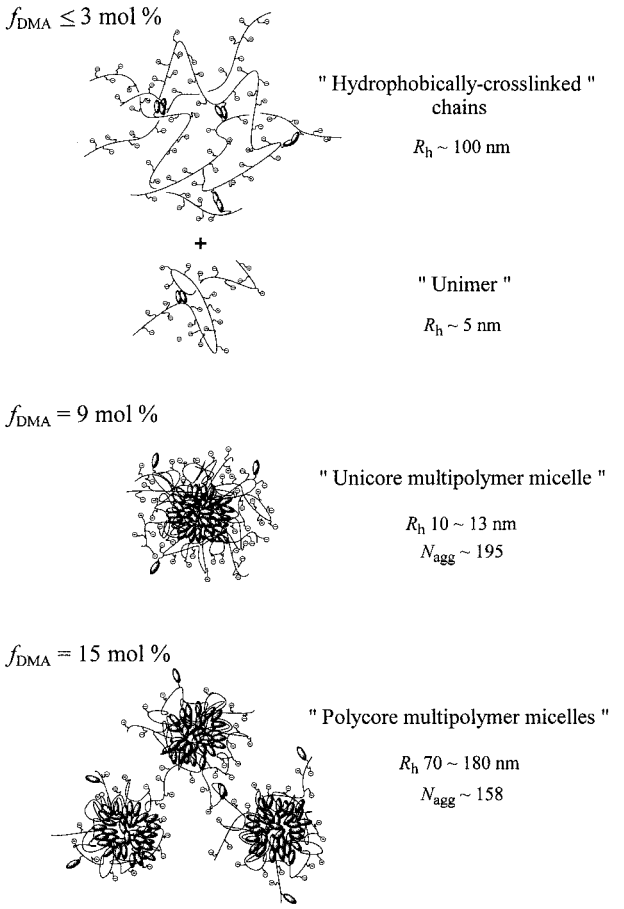

Figure 11. Conceptual illustration of models for multipolymer aggregates.

and *N*-dodecylmethacrylamide (DodMAm),[24,49] although only the difference in these two types of copolymers is the spacer bond connecting dodecyl groups to the polymer backbone (i.e., the ester versus amide bond for the former and the latter, respectively). The solubility of the ester-linked dodecyl copolymers is remarkably different from that of the amide-linked dodecyl copolymers. The ester-linked copolymers are soluble in water only when the DMA contents are lower than 15 mol %, whereas the amide-linked copolymers are soluble in water, giving optically clear aqueous solutions, up to 60 mol % of the DodMAm content.[49] The amide-linked dodecyl copolymers with 10−50 mol % DodMAm contents undergo completely intrapolymer hydrophobe association, forming unimer micelles with hydrodynamic radii ranging from 4 to 6 nm (in 0.05 M NaCl) which remain constant over a wide range of the polymer concentrations.[49a] It should be noted here that values of M_w for these amide-linked copolymers are in a range of $(4-6) \times 10^4$, which are almost the same as those of the ester-linked copolymers in the present study (Table 1).[49] When the DodMAm contents are lower than 10 mol %, however, the amide-linked copolymers undergo interpolymer association at relatively high polymer concentrations (e.g., 5 g/L),[49b] a somewhat similar tendency as that observed for the ester-linked copolymers in the present study.

Association Models for the Copolymers. On the basis of the experimental results, we propose a conceptual model for the hydrophobic association of the AMPS−DMA copolymer as illustrated in Figure 11. The association behavior of the copolymer is strongly dependent on f_{DMA} and may be classified into three types according to f_{DMA}. When $f_{DMA} < 3$ mol %, some polymer chains form multipolymer aggregates with a hydrodynamic radius of about 100 nm while some polymer chains remain as unimers with a hydrodynamic radius of about 5 nm. These multipolymer aggregates may be viewed as an assembly of "hydrophobically cross-linked" polymer chains rather than a polymer micelle. With an increase in the polymer concentration, the fraction of the multipolymer aggregate relative to the unimer increases. When f_{DMA} is increased to 9 mol %, intra- and interpolymer hydrophobe associations lead to the formation of a multipolymer micelle with an apparent mean hydrodynamic radius of 10−13 nm. The N_{agg} of dodecyl groups in a micelle core is more or less 195, independent of the polymer concentration. Because one polymer chain for $f_{DMA} = 9$ mol % has 18 dodecyl units (Table 1), one micelle is formed from at least 11 polymer chains assuming a "unicore" micelle. Considering the size of the polymer micelle ($R_h = 10-13$ nm), "polycore" micelles with a larger number of polymer chains are unrealistic. When f_{DMA} is further increased to 15 mol %, R_h for the multipolymer micelle markedly increases to 70−180 nm, the size increasing with increasing polymer concentration. From the observations that R_h for this copolymer micelle is much larger than that for $f_{DMA} = 9$ mol % whereas N_{agg} for $f_{DMA} = 15$ mol % is a little smaller than that for $f_{DMA} = 9$ mol %, it is reasonable to consider that the polymer micelle for $f_{DMA} = 15$ mol % is a "polycore" micelle made up with a larger number of polymer chains. As depicted in Figure 11, we would assume that this polycore micelle is an assembly of unicore micelle units bridged together, N_{agg} for each unicore micelle unit being about 158 (Table 1).

An important observation in the present study is that the distribution of the hydrodynamic sizes for the multipolymer aggregates, both the hydrophobically cross-linked chains and polymer micelles, is monodisperse (Figure 8). This is particularly true for the micelle formed from the copolymer with $f_{DMA} = 15$ mol %. In other words, the number of polymer chains that can associate to form a polymer micelle is limited. This behavior is in contrast to the general behavior of so-called hydrophobically associating "thickeners" which would form extensive hydrophobic "cross-links", leading to a large increase in the viscosity with an increase in the polymer concentration. For some block copolymers, "superbridges" or "superloops" have been postulated.[50,51] For the AMPS−DMA random copolymers, such superloops may occur to some extent but would be limited because the dodecyl groups are linked to a polyelectrolyte chain, and hydrophobe associations would occur against electrostatic repulsions. Thus, the solution behavior of the AMPS−DMA copolymer is quite different from that of ordinary associating polymers. For all the AMPS−DMA copolymers studied in this work, shear thinning was not observed in the shear rate range of $1-500$ s^{-1} (data not shown), and also their viscosities were found to be very low compared to those of associating polymers.[47,48,52−54]

Conclusions

The hydrophobic association of the random copolymers of AMPS and DMA with f_{DMA} ranging from 1 to 15 mol % was characterized by fluorescence and QELS techniques in 0.1 M NaCl aqueous solutions. Steady-state and time-dependent fluorescence data for pyrene

probes indicate that interpolymer hydrophobic associations begin to occur at a relatively well-defined concentration of the polymer, which is regarded as a "cmc". The cmc strongly depends on f_{DMA}, ranging from 0.019 g/L for $f_{DMA} = 15$ mol % to 9.0 g/L for $f_{DMA} = 1$ mol %. The aggregation numbers of the pendant dodecyl groups were estimated to be about 195 and 158 for $f_{DMA} = 9$ and 15 mol %, respectively, by a time-dependent fluorescence method based on the quenching of pyrene monomeric fluorescence due to excimer formation within a hydrophobic microdomain. QELS data indicated that the association behavior of the copolymer was strongly dependent on f_{DMA}. In the case of $f_{DMA} \leq 3$ mol %, some polymer chains form multipolymer aggregates with $R_h \approx 100$ nm, which arise from "hydrophobic cross-linking" via the interpolymer association of dodecyl groups, while some polymers coexist as unimers with $R_h \approx 5$ nm. For the polymer with $f_{DMA} = 9$ mol %, interpolymer hydrophobe associations lead to the formation of a multipolymer micelle with $R_h \approx 10-13$ nm. For the polymer with $f_{DMA} = 15$ mol %, on the other hand, R_h for the multipolymer micelle markedly increases to 70−180 nm, and the size increases with an increase in the polymer concentration. On the basis of the results from the fluorescence and QELS measurements, a unicore micelle model was proposed for the copolymer with $f_{DMA} = 9$ mol %, and a bridged micelle model was proposed for the copolymer with $f_{DMA} = 15$ mol %.

Acknowledgment. This work was supported in part by a Grant-in-Aid for Scientific Research No. 10450354 from the Ministry of Education, Science, Sports, and Culture, Japan.

References and Notes

(1) Zang, Y. X.; Da, A. H.; Hogen-Esch, T. E.; Butler, G. B. In *Water Soluble Polymers: Synthesis, Solution Properties and Application*; Shalaby, S. W., McCormick, C. L., Butler, G. B., Eds.; ACS Symposium Series 467; American Chemical Society: Washington, DC, 1991; p 159.
(2) Varadaraj, R.; Branham, K. D.; McCormick, C. L.; Bock, J. In *Macromolecular Complexes in Chemistry and Biology*; Dubin, P., Bock, J., Davis, R. M., Schulz, D. N., Thies, C., Eds., Springer-Verlag: Berlin, 1994; p 15 and references therein.
(3) Bock, J.; Varadaraj, R.; Schulz, D. N.; Maurer, J. J. In *Macromolecular Complexes in Chemistry and Biology*; Dubin, P., Bock, J., Davis, R. M., Schulz, D. N., Thies, C., Eds.; Springer-Verlag: Berlin, 1994; p 33 and references therein.
(4) Schmolka, I. R. *J. Am. Oil Chem. Soc.* **1991**, *68*, 206.
(5) Almgren, M.; Bahadur, P.; Jansson, M.; Li, P.; Brown, W.; Bahadur, A. *J. Colloid Interface Sci.* **1991**, *151*, 157.
(6) Malmsten, M.; Lindman, B. *Macromolecules* **1992**, *25*, 5440.
(7) a)Linse, P.; Björling, M. *Macromolecules* **1991**, *24*, 6700. (b) Linse, P.; Malmsten, M. *Macromolecules* **1992**, *25*, 5434. (c) Linse, P. *J. Phys. Chem.* **1993**, *97*, 13896. (d) Linse, P. *Macromolecules* **1993**, *26*, 4437. (e) Linse, P. *Macromolecules* **1994**, *27*, 2685. (f) Malmsten, M.; Linse, P.; Zhang, K.-W. *Macromolecules* **1993**, *26*, 2905.
(8) Webber, S. E. *Chem. Rev.* **1990**, *90*, 1469.
(9) Glatter, O.; Günther, S.; Schilén, K.; Brown, W. *Macromolecules* **1994**, *27*, 6046.
(10) Hurter, P. N.; Scheutjens, J. M. H. M.; Hatton, A T. *Macromolecules* **1993**, *26*, 5592.
(11) Webber, S. E. *J. Phys. Chem. B* **1998**, *102*, 2618.
(12) Chang, Y.; McCormick, C. L. *Macromolecules* **1993**, *26*, 6121.
(13) McCormick, C. L.; Chang, Y. *Macromolecules* **1994**, *27*, 2151.
(14) Kramer, M. C.; Welch, C. G.; Steger, J. R.; McCormick, C. L. *Macromolecules* **1995**, *28*, 5248.
(15) Hu, Y.; Kramer, M. C.; Boudreaux, C. J.; McCormick, C. L. *Macromolecules* **1995**, *28*, 7100.
(16) Branham, K. D.; Snowden, H. S.; McCormick, C. L. *Macromolecules* **1996**, *29*, 254.
(17) Kramer, M. C.; Steger, J. R.; Hu, Y.; McCormick, C. L. *Macromolecules* **1996**, *29*, 1992.
(18) Hu. Y.; Smith, G. L.; Richardson, M. F.; McCormick, C. L. *Macromolecules* **1997**, *30*, 3526.
(19) Hu. Y.; Armentrout, R. S.; McCormick, C. L. *Macromolecules* **1997**, *30*, 3538.
(20) Morishima, Y.; Nomura, S.; Ikeda, T.; Seki, M.; Kamachi, M. *Macromolecules* **1995**, *28*, 2874.
(21) Yusa, S.; Kamachi, M.; Morishima, Y. *Langmuir* **1998**, *14*, 6059.
(22) Morishima, Y. *Trends Polym. Sci.* **1994**, *2*, 31.
(23) Morishima, Y. In *Solvents and Self-Organization of Polymers*; Webber, S. E., Tuzar, D., Munk, P., Eds.; Kluwer Academic Publishers: Dordrecht, The Netherlands, 1996; p 331.
(24) (a) Morishima, Y.; Tominaga, Y.; Kamachi, M.; Okada, T.; Hirata, Y.; Mataga, N. *J. Phys. Chem.* **1991**, *95*, 6027. (b) Morishima, Y.; Tominaga, Y.; Nomura, S.; Kamachi, M. *Macromolecules* **1992**, *25*, 861. (c) Yamamoto, H.; Mizusaki, M.; Yoda, K.; Morishima, Y. *Macromolecules* **1998**, *31*, 3588.
(25) Morishima, Y. *Prog. Polym. Sci.* **1990**, *15*, 949.
(26) Morishima, Y. *Adv. Polym. Sci.* **1992**, *104*, 51.
(27) Morishima, Y. *Bio Ind.* **1995**, *12*, 20.
(28) Morishima, Y.; Seki, M.; Nomura, S.; Kamachi, M. In *Macroion Characterization: From Dilute Solutions to Complex Fluids*; Schmitz, K. S., Ed.; ACS Symposium Series 548; American Chemical Society: Washington, DC, 1994; p 243.
(29) Morishima, Y. In *Multidimensional Spectroscopy of Polymers: Vibrational, NMR, and Fluorescence Techniques*; Urban, M. W., Provder, T., Eds.; ACS Symposium Series 598; American Chemical Society: Washington, DC, 1995; p 490.
(30) Halperin, A. *Macromolecules* **1991**, *24*, 1418.
(31) Semenov, A. N.; Joanny, J.-F.; Khokhlov, A. R. *Macromolecules* **1995**, *28*, 1066.
(32) In *Handbook of Fluorescence Spectra of Aromatic Molecules*; Berlman, I. B., Ed.; Academic Press: New York, 1971.
(33) Wilhelm, M.; Zhao, C.-L.; Wang, Y.; Xu, R.; Winnik, M. A.; Mura, J.-L.; Riess, G.; Croucher, M. D. *Macromolecules* **1991**, *24*, 1033.
(34) (a) Infelta, P. P.; Grätzel, M.; Thomas, J. K. *J. Phys. Chem.* **1974**, *78*, 190. (b)Tachiya, A. M. *Chem. Phys. Lett.* **1975**, *33*, 289. (c) Infelta, P. P. *Chem. Phys. Lett.* **1979**, *61*, 88.
(35) Yekta, A.; Aikawa, M.; Turro, N. J. *Chem. Phys. Lett.* **1979**, *63*, 543.
(36) Yekta, A.; Xu, B.; Duhamel, J.; Adiwidjaja, H.; Winnik, M. A. *Macromolecules* **1995**, *28*, 956.
(37) Xu, B.; Zhang, K.; Macdonald, P. M.; Winnik, M. A.; Jenkins, R. D.; Bassett, D. R.; Wolf, D.; Nuyken, O. *Langmuir* **1997**, *13*, 6896.
(38) Jakes, J. *Czech. J. Phys.* **1988**, *B38*, 1305.
(39) Phillies, G. D. *J. Anal. Chem.* **1990**, *62*, 1049A; *J. Chem. Phys.* **1988**, *89*, 91.
(40) Kalyanasundaram, K.; Thomas, J. K. *J. Am. Chem. Soc.* **1977**, *99*, 2039.
(41) Nakajima, A. *J. Mol. Spectrosc.* **1976**, *61*, 467.
(42) Zana, R. In *Surfactant Solutions: New Methods of Investigation*; Zana, R., Ed.; Marcel Dekker: New York, 1986; pp 241−294.
(43) *Physico-Chemical Properties of Selected Anionic, Cationic and Nonionic Surfactants*; van Os, N. M., Haak, J. R., Rupert, L. A. M., Eds.; Elsevier Science Publishers B. V.: New York, 1993.
(44) Astafieva, I.; Zhong, X. F.; Eisenberg, A. *Macromolecules* **1993**, *26*, 7339.
(45) For example: Aniansson, E. A. G.; Wall, S, N.; Almgren, M.; Hoffman, H.; Kielman, I.; Ulbricht, W.; Zana, R.; Lang, J.; Tondre, C. *J. Phys. Chem.* **1976**, *80*, 905.
(46) For example: Chang, J. N.; Kaler, E. W. *J. Phys. Chem.* **1985**, *89*, 2996. Corti, M.; Degiorgio, V. *J. Phys. Chem.* **1981**, *85*, 711.
(47) Hayter, J. B.; Penfold, *J. Colloid Polym. Sci.* **1983**, *261*, 1022.
(48) For example: (a) Lianos, P.; Zana, R. *J. Colloid Interface Sci.* **1981**, *84*, 100. (b) Almgren, M.; Löfroth, J. E. *J. Colloid Interface Sci.* **1981**, *81*, 486. (c) Turro, N. J.; Yekta, A. *J. Am. Chem. Soc.* **1978**, *100*, 5951. (d) Croonen, Y,; Geladé, E.; Zegel, van der M.; Auweraer, van der M.; Vandendriessche, H.; Schryver, de F. C.; Almgren M. *J. Phys. Chem.* **1983**, *87*, 1426.

(49) (a) Yamamoto, H.; Morishima, Y., to be published. (b) Hashidzume, A.; Yamamoto, H.; Mizusaki, M.; Morishima, Y. *Polym. J.*, in press.
(50) Alami, E.; Almgren, M.; Brown, W. *Macromolecules* **1996**, *29*, 2229.
(51) Annable, T.; Buscall, R.; Ettelaie, R.; Whittlestone, D. *J. Rheol.* **1993**, *37* (4), 695.
(52) Kumacheva, E.; Rharbi, Y.; Winnik, M. A.; Guo, L.; Tam, K. C.; Jenkins, R. D. *Langmuir* **1997**, *13*, 182.
(53) Tam, K. C.; Jenkins, R. D.; Winnik, M. A.; Bassett, D. R. *Macromolecules* **1998**, *31*, 4149.
(54) Xu, B.; Yekta, A.; Winnik, M. A.; Sadeghy-Dalivand, K.; James, D. F.; Jenkins, R. D.; Bassett, D. R. *Langmuir* **1997**, *13*, 6903.

MA990202J